



Predicted cross sections for the synthesis of $Z = 120$ fusion via $^{54}\text{Cr} + ^{248}\text{Cm}$ and $^{50}\text{Ti} + ^{249}\text{Cf}$ target-projectile combinations

Sahila Chopra ¹ and Peter O. Hess ^{1,2}¹*Frankfurt Institute for Advanced Studies (FIAS), D-60438 Frankfurt am Main, Germany*²*Instituto de Ciencias Nucleares, UNAM, 04510 Mexico-City, Mexico*

(Received 29 March 2024; accepted 26 June 2024; published 11 July 2024)

The production of superheavy elements (SHE) is confronted with significant experimental difficulties owing to extremely low cross sections for their formation in heavy-ion fusion reactions. Accurate predictions of these cross sections along with the corresponding excitation functions are of the utmost importance for future experiments. Theoretical studies are needed in order to investigate the decay properties of excited SHE. A recent conclusion on the importance of the neck-length parameter [S. Chopra, N. Goel, M. K. Sharma, P. O. Hess, and Hemdeep, *Phys. Rev. C* **106**, L031601 (2022)] within the framework of the dynamical cluster-decay model (DCM) became foundational for this work, which explained the ability of the DCM to predict the decay cross sections in hot fusion reactions. The model is a nonstatistical description for the decay of a compound nucleus (CN). The only parameter of the model is the neck-length parameter, which is related to the total kinetic energy $\text{TKE}(T)$ or the effective Q value $Q_{\text{eff}}(T)$ at the temperature T of the CN. This work shows that the hot fusion reactions $^{54}\text{Cr} + ^{248}\text{Cm}$ and $^{50}\text{Ti} + ^{249}\text{Cf}$, in the decay of $4n$ evaporation channel may be more favorable for the synthesis of the $Z = 120$ SHE. After the emission of four neutrons, $^{302}120^*$ can reach $^{298}120$ and this would lead to the formation of $^{294}118$ after one α decay. In the same way, $^{50}\text{Ti} + ^{249}\text{Cf}$ can end up at some known nuclei. If this happens, it would be a positive sign for the synthesis of $Z = 120$ from one of these two nuclear reactions. The present work calculated the cross sections of all possible decay modes, i.e., evaporation residues, fission, and quasifission for the chosen reactions. In addition, an evaluation for the total or capture cross section is applied, for the case of $Z = 120$, without the use of any input of a single experimental data. These predictions may be useful for upcoming experiments.

DOI: [10.1103/PhysRevC.110.014615](https://doi.org/10.1103/PhysRevC.110.014615)

I. INTRODUCTION

Experimentally and theoretically, It is still an open question as to how to synthesize the elements $Z = 119$ and 120 . According to theoretical predictions, the island of stability is believed to be near the neutron shell at $N = 184$ and proton shells at $Z = 120$ – 126 . For the synthesis of $Z = 120$, various theoretical predictions have been made with different target and projectile combinations and a few experiments have also been attempted in the last decade in different laboratories. However, no events have been recorded yet. Experimentally, $Z = 107$ – 112 were successfully synthesized at GSI in cold fusion reactions using ^{208}Pb and ^{209}Bi targets [1,2]. Hofmann and his group also made efforts to synthesize $Z = 120$ using a $^{54}\text{Cr} + ^{248}\text{Cm}$ reaction without success [3]. Despite that we have chosen the $^{54}\text{Cr} + ^{248}\text{Cm}$ reaction to study in this work. Currently experiments to synthesize $Z = 120$ are underway, but due to a low cross section, no success has been achieved yet. The $^{54}\text{Cr} + ^{248}\text{Cm}$ reaction was investigated at the velocity filter SHIP at GSI, Darmstadt, Germany. In that experiment only a one-event limit cross section was observed around 500 fb. If this reaction does not produce the expected results, then it has to search for another one. In this context, numerous studies are available in which elements $Z = 119$ and 120 were investigated using different targets and

projectiles. As, in Ref. [4], it has been discussed that there are possible chances for the synthesis of $Z = 120$ using the titanium beam. Some other theories and experimental attempts also support this result in the case of the Ti beam. In Ref. [5], the formation of $Z = 120$ has been studied forming with the Ti-induced reaction using the dinuclear system (DNS) model. The DNS was also proven to be reliable in describing the production of new superheavy elements (SHE) [6,7]. Reference [8] discussed an output from the experiment using the pulsed beams of ^{64}Ni , ^{58}Fe , ^{54}Cr , and ^{50}Ti performed at the Heavy Ion Accelerator Facility operated by the Australian National University in Canberra, Australia. The results from this experiment were also supported by a Ti beam for the synthesis of 120 . Another four-month long experiment with a high-intensity ^{50}Ti beam bombarding $^{249}\text{Bk}/^{249}\text{Cf}$ targets was carried out successfully at the gas-filled recoil separator TASCA [9]. According to the experimental observations, the Ti beam could be considered for the synthesis of future SHEs, 119 and 120 . So, our second reaction taken under consideration is the Ti-induced reaction for a comparative study with a Cr-induced reaction. Our ideas have been proposed for the synthesis of $Z = 120$ only, from $^{54}\text{Cr} + ^{248}\text{Cm}$ and $^{50}\text{Ti} + ^{249}\text{Cf}$ reactions with the expected cross sections within the limit of experimental possibilities. In the present contribution for cross section calculations, the decided range

of the excitation energy (E^*) is from 35–50 MeV. The purpose of taking this energy range is the proposal from GSI experimentalists about the possibilities that this reaction may happen in this range of energy. A specific criterion has been followed in this work to calculate the decay cross sections, i.e., using the same potential barriers for both reactions with exactly the same neck-length parameter (ΔR) values. In the present contribution we apply the dynamical cluster-decay model (DCM), using the framework of a non-coplanar configuration and including up to the hexadecapole deformations. Here, the important question is: Are Ca-induced reactions compatible to produce $Z = 120$? Experimentally, a reason is being given for small chances of the production of $Z = 119$ and 120 using ^{48}Ca , i.e., to synthesize $Z = 120$ with ^{48}Ca , it is necessary to react with einsteinium targets ($Z = 100$). But, they are very radioactive and only available in very small and limited amounts, which is not favorable for the synthesis of superheavy elements. Therefore, the heaviest targets are Cm, Bk, and Cf, which need to be combined with heavier projectiles than ^{48}Ca to get $Z = 119$ and 120. Due to these arguments, nuclear reactions considered for this study are Cr and Ti induced. The important question regarding the model predictions is: To what extent and how precisely can the cross sections for new super heavy elements be predicted? In order to answer this question we have tested the capability of our model to make predictions with respect to the case of new upcoming compound nuclei [10].

However, it is difficult to make any statement without experimental verifications. In this contribution, ideas have also been taken from the previously studied superheavy elements using the DCM. To estimate the cross sections in case of SHE, one needs to understand the concept of different decay modes, evaporation residues (ER or LPs), fusion-fission (ff), and quasifission (qf), i.e., the light particles (LPs, $A \leq 4$), fusion-fission fragments (ff; $A/2 \pm 20$), and the quasifission defined for the incoming channel since the target and projectile nuclei can be considered to have not yet lost their identity. In the case of superheavy elements, a significantly larger production rate of qf and ff than the ERs has been observed. Therefore, our main focus is to calculate the possible cross sections of qf and ff along with the evaporation residues. We will present simultaneous calculations of all decay channels. ΔR is also known as a reaction-time scale, because it explains the time of occurrence (earlier or later) of different decay modes (ER, ff and qf) of a compound nucleus.

The main objective of this paper is to obtain realistic predictions for decay modes of SHE using the DCM. We have considered four energies for both reactions within the range of 35 to 50 MeV, namely $E^* = 35, 40, 45, \text{ and } 50$ MeV. Performing a theoretical calculation without any experimental data is a challenge. This work has been done using the non-coplanar degrees of freedom ($\Phi_c \neq 0^\circ$) within the DCM composition. These calculations are more time consuming than coplanar ($\Phi_c = 0^\circ$) configurations but more reliable. For these calculations, the foremost task is to choose the appropriate values of the neck-length parameter for different decay channels, i.e., ER, ff, and qf. In this work, efforts for the calculations are dependent on the previous results using the DCM, especially in the case of superheavy elements [10,11]. In a previous pub-

lication [12], the studied reaction was $^{54}\text{Cr} + ^{248}\text{Cm}$ for the synthesis of $Z = 120$ within the substructure of the coplanar degree of freedom ($\Phi = 0^\circ$) using the DCM. In this model, the choice of degrees of-, i.e., coplanar ($\Phi = 0^\circ$) or non-coplanar ($\Phi_c \neq 0^\circ$) configuration is also very crucial. In the present study we are dealing with $\Phi_c \neq 0^\circ$ which provided better results than $\Phi = 0^\circ$ and moves the calculations closer to the natural output of a nuclear reaction [13].

There are different types of phenomenological models to describe the reaction dynamics of heavy ions. The present most widespread models are the dinuclear system (DNS) model [7] and an adiabatic model which is based on a stochastic approach and Langevin-type dynamical equations of motion [14], both developed substantially at the Joint Institute for Nuclear Research JINR Dubna (Russia). These are statistical models based on the CN fusion probability P_{CN} and the CN survival probability P_{surv} . Nevertheless, the DCM is equally capable of determining the individual contributions of all decay cross sections as well as mass and energy distributions of the reaction products.

The article is organized as follows. Section II gives a brief description of the dynamical cluster-decay model (DCM). Our calculations for the $^{54}\text{Cr} + ^{248}\text{Cm}$ and $^{50}\text{Ti} + ^{249}\text{Cf}$ reactions, using deformed and non-coplanar oriented nuclei, are presented in Sec. III. In Sec. IV, conclusions are drawn.

II. THE MODEL

The DCM established by Greiner, Gupta, and collaborators (see, e.g., the reviews [15,16]) is a reformulation of the preformed cluster-decay model (PCM). The PCM is specially suited for the study of cluster radioactivity (heavy-ion radioactivity) and α decay by heavy nuclei. It was introduced in the early 1980s by Sandulescu, Poenaru, and Greiner [17]. The DCM model is based on the collective coordinates of mass (and charge) asymmetries η (and η_Z) [$\eta = (A_1 - A_2)/(A_1 + A_2)$, $\eta_Z = (Z_1 - Z_2)/(Z_1 + Z_2)$], and the relative separation R with multipole deformations $\beta_{\lambda i}$ ($\lambda = 2,3,4$; $i = 1,2$), orientations θ_i , and the azimuthal angle Φ between the principal planes of two nuclei (see Fig. 1, where only the lower halves of the two nuclei are shown [18]). We investigate the transfer of kinetic energy from the incident channel $E_{c.m.}$ to internal excitation [total excitation energy (TXE) or total kinetic energy (TKE)] of the outgoing channel, since a particular value of neck-length parameter (ΔR), at which the process is calculated, depends on the temperature T as well as on η , i.e., $R(T, \eta)$.

T , the nuclear temperature, is related to the excitation energy via

$$E^* = (A/a)T^2 - T \quad (\text{in MeV}) \quad (1)$$

with the level density parameter $a = 11$ MeV for SHE (for others $a = 8$ MeV, 9 MeV) depending on the mass A of the CN. Further, the DCM, extended to include deformation and orientation effects of the two incoming or outgoing nuclei, also contains the effects of angular momentum ℓ and temperature T .

In terms of these coordinates, for ℓ partial waves, we define the compound nucleus decay cross section for each

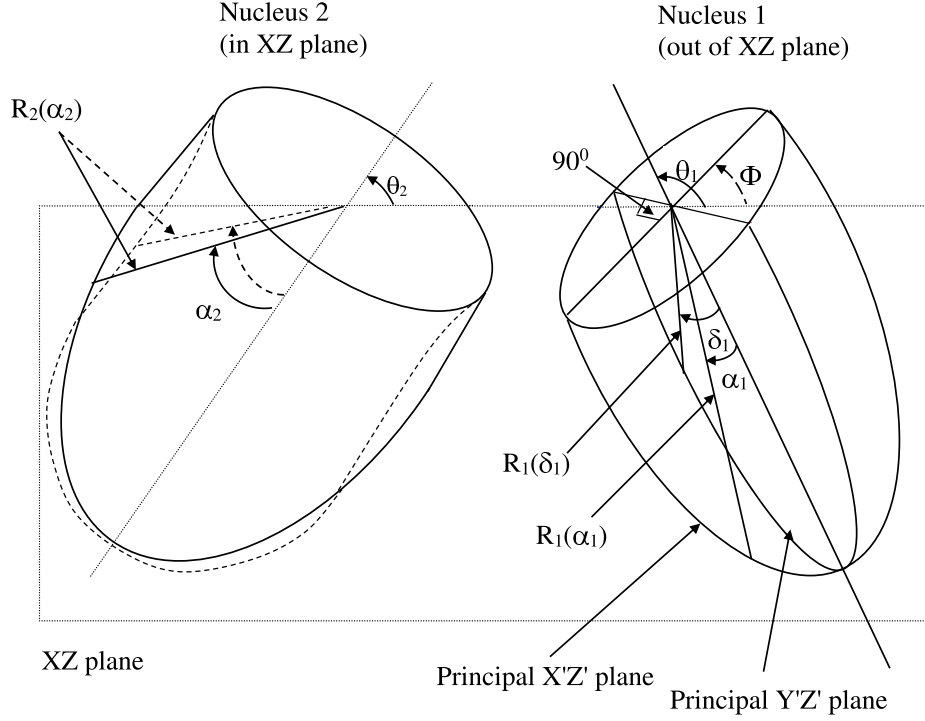


FIG. 1. Two unequal nuclei are depicted, oriented at angles θ_1 and θ_2 , with their principal planes $X'Z'$ and XZ with an azimuthal angle Φ . The angle Φ is shown by a dashed line, since it is an angle coming out of the plane XZ . Nucleus 2 is in the XZ plane and for the out-of-plane nucleus 1 another principal plane $Y'Z'$, perpendicular to $X'Z'$, is also shown. The orientation angles θ_i are measured counterclockwise from the collision Z axis, and the angles α_i (and δ_i) of radius vectors are measured in the clockwise direction from the nuclear symmetry axis.

fragmentation as

$$\sigma_{(A_1, A_2)} = \frac{\pi}{k^2} \sum_{\ell=0}^{\ell_{\max}} (2\ell + 1) P_0 P; \quad k = \sqrt{\frac{2\mu E_{c.m.}}{\hbar^2}}, \quad (2)$$

where P_0 is the preformation probability referring to the η motion and P , the penetrability, to the R motion, both dependent on angular momentum ℓ and temperature T . μ is the reduced mass. ℓ_{\max} is the maximum angular momentum, defined for the light particle evaporation residue cross section $\sigma_{ER} \rightarrow 0$. The same formula is applicable to the noncompound-nucleus (nCN) decay process, calculated as the quasifission (qf) decay channel, where $P_0 = 1$ for the incoming channel since the target and projectile nuclei can be considered to have not yet lost their identity. Thus, for P calculated for the *incoming channel* η_{ic} , we have

$$\sigma_{nCN} = \frac{\pi}{k^2} \sum_{\ell=0}^{\ell_{\max}} (2\ell + 1) P_{\eta_{ic}}. \quad (3)$$

Note that Eq. (2) is defined in terms of the exit and/or decay channels alone, i.e., both the formation P_0 and then their emission via barrier penetration P are calculated only for the decay channels (A_1, A_2) . It follows from Eq. (2) that

$$\sigma_{ER} = \sum_{A_2=1}^{40F5} \sigma_{(A_1, A_2)} \text{ or } = \sum_{x=1}^{40F5} \sigma_{xn} \quad (4)$$

and

$$\sigma_{ff} = 2 \sum_{A/2-x}^{A/2} \sigma_{(A_1, A_2)}, \quad (5)$$

where σ_{ff} should be multiplied by a factor of 2, i.e., on both sides of the fragmentation in the heavy and low mass regions.

P_0 is the solution of the stationary Schrödinger equation in η at a fixed $R = R_a$ and the equation to be resolved is

$$\left\{ -\frac{\hbar^2}{2\sqrt{B_{\eta\eta}}} \frac{\partial}{\partial \eta} \frac{1}{\sqrt{B_{\eta\eta}}} \frac{\partial}{\partial \eta} + V(R, \eta, T) \right\} \psi^v(\eta) = E^v \psi^v(\eta) \quad (6)$$

with $v = 0, 1, 2, 3, \dots$ referring to ground-state ($v = 0$) and excited-state solutions. The probability P_0 is given by

$$P_0(A_i) = |\psi(\eta(A_i))|^2 \sqrt{B_{\eta\eta}} \frac{2}{A}, \quad (7)$$

where we use, for $|\psi|^2$, a Boltzmann-like function,

$$|\psi|^2 = \sum_{v=0}^{\infty} |\psi^v|^2 \exp(-E^v/T). \quad (8)$$

For the position $R = R_a$, the first turning point for calculating the penetration P in the decay of a hot CN, we use the postulate [19–21]

$$\begin{aligned} R_a(T) &= R_1(\alpha_1, T) + R_2(\alpha_2, T) + \Delta R(\eta, T), \\ &= R_r(\alpha, \eta, T) + \Delta R(\eta, T) \end{aligned} \quad (9)$$

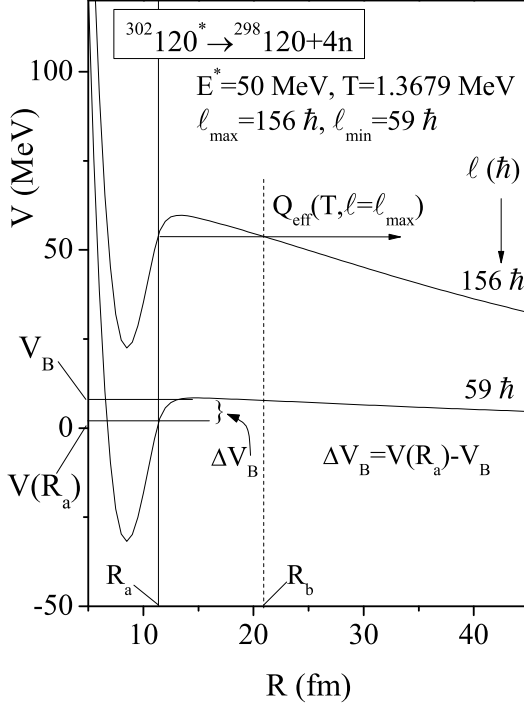


FIG. 2. The ℓ -dependent scattering potential $V(R)$ for $^{302}\text{120} + 4n$, in the decay of $^{302}\text{120}^*$ is formed in the $^{54}\text{Cr} + ^{248}\text{Cm}$ reaction at $E^* = 50$ MeV. The concept of barrier lowering $\Delta V_B = V(R_a) - V_B$ is also shown in this figure for the $\ell_{\max} = 156\hbar$ and $\ell_{\min} = 59\hbar$ values. The first and second turning points are denoted by R_a and R_b , respectively.

with radius vectors

$$R_i(\alpha_i, T) = R_{0i}(T) \left[1 + \sum_{\lambda} \beta_{\lambda i} Y_{\lambda}^{(0)}(\alpha_i) \right] \quad (10)$$

and temperature-dependent nuclear radii $R_{0i}(T)$ for the equivalent spherical nuclei [22],

$$R_{0i} = [1.28A_i^{1/3} - 0.76 + 0.8A_i^{-1/3}](1 + 0.0007T^2). \quad (11)$$

The only parameter of the model $\Delta R(T)$, the neck-length parameter, is T dependent, defining the first turning point R_a in Eq. (9). $\Delta R(\eta, T)$ assimilates the deformation and neck formation effects between the two nuclei, introduced within the extended model of Gupta and collaborators [23–25]. This method of introducing a neck-length parameter ΔR is similar to that used in both the scission-point [26] and saddle-point [27,28] statistical fission models.

The choice of the parameter R_a (equivalently, ΔR) in Eq. (9), for a best fit to the data, allows us to relate in a simple way the $V(R_a, \ell)$ to the top of the barrier $V_B(\ell)$ for each ℓ , by defining their difference $\Delta V_B(\ell)$ as the effective “lowering of the barrier”,

$$\Delta V_B(\ell) = V(R_a, \ell) - V_B(\ell). \quad (12)$$

Note that ΔV_B for each ℓ is defined as a negative quantity since the actually used barrier is effectively lowered. This is illustrated in Fig. 2 for the ℓ_{\max} value, which is fixed for the light-particle (here, e.g., x neutrons xn , $x = 1-4$) cross section

$\sigma_{xn}(\ell) \rightarrow 0$, owing to $P_0 \rightarrow 0$, or for ff the P_0 approaches a (nearly) constant maximum value. Thus, the fitting parameter ΔR controls the “barrier lowering” ΔV_B .

The collective fragmentation potential $V_R(\eta, T)$ is given below in Eq. (13) and includes the structure effects of the CN into the formalism. It is calculated according to the Strutinsky renormalization procedure ($B = V_{LDM} + \delta U$; B is binding energy), namely,

$$\begin{aligned} V_R(\eta, T) = & - \sum_{i=1}^2 [V_{LDM}(A_i, Z_i, T)] \\ & + \sum_{i=1}^2 [\delta U_i] \exp\left(-\frac{T^2}{T_0^2}\right) + V_P(R, A_i, \beta_{\lambda i}, \theta_i, \Phi, T) \\ & + V_C(R, Z_i, \beta_{\lambda i}, \theta_i, \Phi, T) \\ & + V_{\ell}(R, A_i, \beta_{\lambda i}, \theta_i, \Phi, T), \end{aligned} \quad (13)$$

where V_C , V_P , and V_{ℓ} are the Coulomb, nuclear proximity, and angular momentum dependent potentials for deformed, oriented (coplanar or non-coplanar) nuclei, all T -dependent. For V_P , we use the pocket formula of Blocki *et al.* [29], and in $V_{\ell}(T) [= \hbar^2 \ell(\ell + 1)/2I(T)]$, the moment of inertia I is taken in the complete sticking limit $I = I_S(T) = \mu R^2 + \frac{2}{5}A_1 m R_1^2(\alpha_1, T) + \frac{2}{5}A_2 m R_2^2(\alpha_2, T)$. In general, the experimental numbers for ℓ are based on the moment of inertia calculated in the nonsticking limit $I = I_{NS} = \mu R^2$. We find that in the sticking limit, I_S used here is more appropriate for the proximity potential (with nuclear surfaces ≤ 2 fm apart) which has as a consequence a much larger ℓ value. For nuclear collisions, the use of a larger ℓ_{\max} value, due to relatively larger magnitude of I_S , is shown [30] to result in the reduction of the nuclear surface separation distances ΔR and vice versa for I_{NS} .

A. Framework for non-coplanar nuclei

To calculate the cross sections for non-coplanar nuclei ($\Phi \neq 0^\circ$), we use the same formalism as for $\Phi = 0^\circ$ (see Ref. [31]), but by replacing for the out-of-plane nucleus ($i = 1$ or 2) the corresponding radius parameter $R_i(\alpha_i)$ by its projected radius parameter $R_i^P(\alpha_i)$ in both the Coulomb and proximity potentials [18]. For the Coulomb potential, it enters via $R_i(\alpha_i)$ itself, and for the proximity potential via the definitions of both the mean curvature radius \bar{R} and the shortest distance s_0 , i.e., compact configurations with orientations θ_{ci} and Φ_c [32,33]. For compact configurations, the interaction radius is smallest and the barrier is highest.

The $R_i^P(\alpha_i)$ is determined by defining, for the out-of-plane nucleus, two principal planes $X'Z'$ and $Y'Z'$, respectively, with radius parameters $R_i(\alpha_i)$ and $R_j(\delta_j)$, such that their projections into the plane (XZ) of the other nucleus are (see Fig. 1)

$$R_i^P(\alpha_i) = R_i(\alpha_i) \cos \Phi \quad i=1 \text{ or } 2 \quad (14)$$

and

$$R_j^P(\delta_j) = R_j(\delta_j) \cos(\Phi - \delta_j) \quad j = i = 1 \text{ or } 2. \quad (15)$$

Maximizing $R_j(\delta_j)$ with respect to the angle δ_j , we obtain

$$\begin{aligned} R_i^p(\alpha_i) &= R_i^p(\alpha_i = 0^0) + R_i^p(\alpha_i \neq 0^0) \\ &= R_j^p(\delta_j^{\max}) + R_i(\alpha_i \neq 0^0) \cos \Phi \end{aligned} \quad (16)$$

with δ_j^{\max} given by the condition (for fixed Φ)

$$\tan(\Phi - \delta_j) = -\frac{R_j'(\delta_j)}{R_j(\delta_j)}. \quad (17)$$

Thus, the Φ dependence of the projected radius vector $R_i^p(\alpha_i)$ is also contained in the maximized $R_j^p(\delta_j^{\max})$. For further details, see [18]. The nuclear proximity potential denoted by V_P^{12} the potential for nucleus 1 to be out-of-plane and by V_P^{21} for nucleus 2 to be out of plane, the effective nuclear proximity potential is given by

$$V_P = \frac{1}{2}[V_P^{12} + V_P^{21}]. \quad (18)$$

The penetrability P in Eq. (1) or (2) is obtained through the WKB integral

$$P = \exp\left(-\frac{2}{\hbar} \int_{R_a}^{R_b} \{2\mu[V(R, T) - Q_{\text{eff}}]\}^{1/2} dR\right), \quad (19)$$

It is solved analytically [34,35] with the second turning point R_b (see Fig. 2) satisfying

$$V(R_a) = V(R_b) = Q_{\text{eff}}. \quad (20)$$

As the ℓ value increases, the $Q_{\text{eff}}(T)$ increases and hence $V(R_a, \ell)$ increases, too. Thus, R_a acts like a parameter through $\Delta R(\eta, T)$, and we assume that R_a is the same for all ℓ values, i.e., $V(R_a) = Q_{\text{eff}}(T, \ell = 0)$. This is required because we do not know how to add the ℓ effects to the binding energies.

Finally, the compound nucleus formation probability P_{CN} in the case of superheavy elements is defined as

$$P_{CN} = \frac{\sigma_{CN}}{\sigma_{\text{capture}}} = 1 - \frac{\sigma_{qf}}{\sigma_{\text{capture}}}, \quad (21)$$

where $\sigma_{CN} = \sigma_{ER} + \sigma_{ff}$ and $\sigma_{\text{capture}} = \sigma_{qf} + \sigma_{ER} + \sigma_{ff}$. Note, to estimate P_{CN} in the case of light and heavy nuclei, terminologies for contributing cross sections are different for the superheavy elements (see Ref. [36]).

III. RESULTS AND DISCUSSIONS

In this section, ΔR is increased in a certain pattern for three-neutrons ($3n$), four-neutrons ($4n$), and fission region ($A/2 \pm 20$) with the increasing energy values for both the compound nuclei, i.e., $^{302}120^*$ and $^{299}120^*$. The $3n$ and $4n$ decay fragments are high-lighted as per the experimental requirements. Other decay channels simultaneously adjusted themselves accordingly at different ΔR values. Here, the calculations are performed at five excitation energies (E^*) for deformations including up to hexadecapole deformations (β_2 - β_4) and with compact orientations θ_{ci} , $i = 1, 2$, of non-coplanar nuclei (azimuthal angle $\Phi_c \neq 0^\circ$).

A. Analysis of σ_{ER}

We have worked under the assumption that after the emission of $4n$, $^{302}120^*$ will become $^{298}120$ which will

TABLE I. DCM-predicted cross sections at $E^* = 50$ MeV, considering only $4n$ at higher ΔR than other decay channels.

Decay channels –	$\Delta R(\text{fm})$	$\sigma_{ER}^{\text{predicted}}$ (pb)
1n	–0.25	–
2n	–0.25	–
3n	0.5	4.47×10^{-15}
4n	1.5	0.017

end up as $^{294}118$ (a known nucleus) after the single α decay. Similarly, if $^{299}120^*$ also ends at any known nucleus, the possibility of its synthesis may also increase. To start the theoretical calculations, one needs the theoretical understanding of such decay modes, i.e., α decay and decay via evaporation residues or fission decay in order to synthesize possible superheavy elements. Figure 1 of Ref. [37] explains the possible decay modes to reach the known nuclei via different decay modes. First, we have determined the ΔR for the case of $^{54}\text{Cr} + ^{248}\text{Cm}$. Then we have calculated the cross sections with the same ΔR s for another reaction, i.e., $^{50}\text{Ti} + ^{249}\text{Cf}$. In the case of $Z = 122$ [38] using the DCM, exactly the same approach of the calculations was taken under consideration for a comparative study of one nucleus fusing via two different incoming target-projectile combinations.

After the emission of $4n$ from both the considered nuclei, chances for the production of $Z = 120$ may increase. Taking this fact into account, σ_{3n} and σ_{4n} have been calculated with a higher probability than other evaporation residues. Our main focus is on the $4n$ decay but if we restrict ΔR at a very low value for $3n$ then the cross section of $4n$ is very senseless which is not acceptable according to the experimental possibilities (see magnitude differences in Table I only for $^{302}120^*$). Therefore, we have discarded this pattern for the present calculations. The main purpose of Table I is to give an idea about the effect of ΔR , i.e., how does ΔR affect the cross section values up to a limit of other decay channels, even if there is a change for a single fragment. The change in the magnitudes of the cross sections after adjusting the values of ΔR becomes obvious, see Table II.

Therefore, for both nuclear reactions, $3n$ decay has been considered at some logical neck-length value in such a way that it supports the $4n$ decay to get the realistic cross sections at all energies. As is mentioned in several contributions of the DCM, the ΔR parameter is very sensitive up to four-decimal digits [11,38–40]. Moreover the ΔR for different decay fragments can easily affect each others cross sections. Thus, the dynamical cluster-decay model always encourages simultaneous calculations. As the potential barriers were fixed for $3n$ and $4n$, automatically all ΔR s of other decay channels fall into the same pattern, as we have seen so far in most of the cases. The first main point to start the calculations is to choose an acceptable value for the neck-length parameter. Therefore, at all five energies we kept the highest possible one and allowed a value of ΔR within the proximity limits (~ 2 fm) only for $3n$ and $4n$. The rest of the decay fragments will move

TABLE II. This table lists the DCM-predicted cross section ($\sigma_{ER}^{\text{pred.}}$) from the evaporation residues (ER; $A = 1-4$), for best fitted ΔR 's without any experimental data at four E^* 's. We choose $\Phi \neq 0^\circ$ in the pocket formula for the nuclear proximity potential. The neck-length parameters for Cr-induced and Ti-induced reactions are ΔR_{Cr} and ΔR_{Ti} , respectively.

Cr induced; $E^* = 50$ MeV, $E_{c.m.} = 257.61$ MeV, $T = 1.3679$ MeV				
Ti induced; $E^* = 50$ MeV, $E_{c.m.} = 245.97$ MeV, $T = 1.3748$ MeV				
Decay channel	ΔR_{Cr} (fm)	$\sigma_{ER}^{\text{pred.}}$ (pb)	ΔR_{Ti} (fm)	$\sigma_{ER}^{\text{pred.}}$ (pb)
1n	-0.25	—	-0.25	—
2n	-0.25	—	-0.25	—
3n	1.1	3.09×10^{-4}	1.1	1.98×10^{-3}
4n	1.6	5.27×10^{-2}	1.6	0.583
Cr induced; $E^* = 45$ MeV, $E_{c.m.} = 252.61$ MeV, $T = 1.2986$ MeV				
Ti induced; $E^* = 45$ MeV, $E_{c.m.} = 240.97$ MeV, $T = 1.3052$ MeV				
1n	-0.25	—	-0.25	—
2n	-0.25	—	-0.25	—
3n	1.09	1.20×10^{-4}	1.09	7.54×10^{-4}
4n	1.55	1.34×10^{-2}	1.55	0.18
Cr induced; $E^* = 40$ MeV, $E_{c.m.} = 247.61$ MeV, $T = 1.2254$ MeV				
Ti induced; $E^* = 40$ MeV, $E_{c.m.} = 235.97$ MeV, $T = 1.2316$ MeV				
1n	-0.25	—	-0.25	—
2n	-0.25	—	-0.25	—
3n	1.07	2.78×10^{-5}	1.07	2.8×10^{-4}
4n	1.52	4.43×10^{-3}	1.52	6.28×10^{-2}
Cr induced; $E^* = 35$ MeV, $E_{c.m.} = 242.61$ MeV, $T = 1.1474$ MeV				
Ti induced; $E^* = 35$ MeV, $E_{c.m.} = 230.97$ MeV, $T = 1.1533$ MeV				
1n	-0.25	—	-0.25	—
2n	-0.25	—	-0.25	—
3n	1.05	5.68×10^{-6}	1.05	3.03×10^{-5}
4n	1.5	1.59×10^{-3}	1.5	2.21×10^{-2}

under the influence of a collective potential of the system and adjust themselves for different ΔR values accordingly.

In Fig. 3, for both nuclei, ℓ_{max} values are shown at $E^* = 50$ MeV around $156\hbar$ and $168\hbar$. To fix this ℓ_{max} value, evaporation residues were considered along with the contribution of $A_2 = 135$ (from the fission region). This value of ℓ_{max} is the limiting value, although it is very high. However, the ℓ_{max} values for the two decay channels ER and ff are fixed for $P_0 \rightarrow 0$ and acquire a maximum with a (nearly) constant value, respectively, as is illustrated in Fig. 3.

Table II and Fig. 4, present the DCM-predicted ER cross section $\sigma_{ER}^{\text{predicted}}$ (equivalently, $\sigma_{3n,4n}^{\text{predicted}}$), at all energies for both Cr-induced and Ti-induced reactions. Initially, take note of the details of the fits obtained particularly for 3n and 4n with a higher value of ΔR than 1n and 2n (at a negative value of ΔR). Our main focus concerns the 4n channel, along with the fission region because in the matter of superheavy elements, 1n and 2n contributions are not very crucial. However, the decay of 3n is intrusive (as mentioned above) in these cases. Here, the noticeable point is the variation of the ΔR values for different decay channels (ER, ff, and qf) at four energies. In most of the studies within the framework of the

DCM a certain pattern of ΔR has been observed, which is largest for the ER, smaller for the competing quasifission (qf), and smallest for the fusion-fission (ff) of the CN. Therefore, the same trend was observed in the present work, which is already introduced by the previously studied superheavy elements (mentioned in the Introduction). As discussed, the evaporation residues pattern of ΔR , i.e., 4n, dominates, compared to all other decay fragments. The foremost point to note here is the outcome of σ_{ER} in the event of both reactions at the same potential barriers. The cross section magnitude is higher for the $^{50}\text{Ti} + ^{249}\text{Cf}$ than the $^{54}\text{Cr} + ^{248}\text{Cm}$ target-projectile (t-p) combination. Only on the basis of this result is it difficult to say which t-p combination is more likely to be able to synthesize $Z = 120$. So the activity of other decay channels is also important here, e.g., fission and quasifission cross sections.

Note, in a previous publication by us [12], for the study of $Z = 120$ formed via the $^{54}\text{Cr} + ^{248}\text{Cm}$ reaction, there is a mistake committed in writing the mass numbers in the reaction indicated in Table I. In Ref. [12], we have studied the same t-p combination for the synthesis of $Z = 120$ but within the configuration of the coplanar degree of

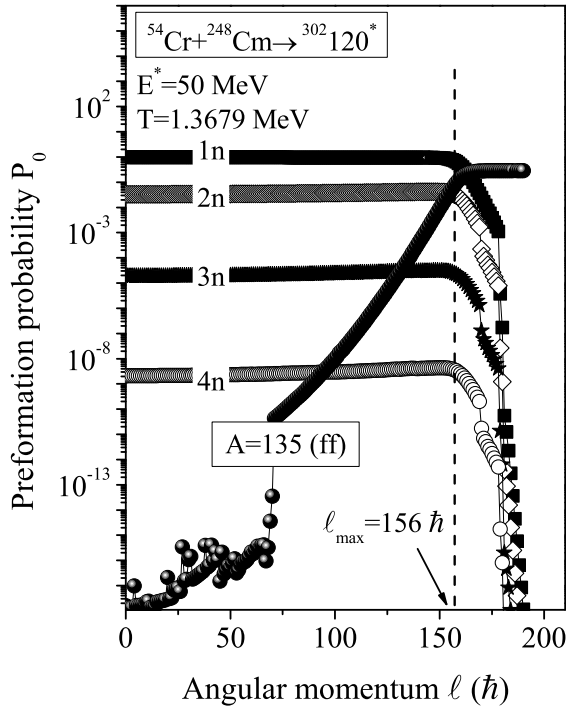


FIG. 3. Preformation probability P_0 as a function of angular momentum ℓ for the ER-decay channels and one fragment from the ff region, i.e., $A_2 = 135$ of $^{302}120^*$ formed in the $^{54}\text{Cr} + ^{248}\text{Cm}$ reaction at $E^* = 50$ MeV. $P_0 \sim 10^{-20}$, which fixes the ℓ_{max} to $156\hbar$.

freedom ($\Phi_c = 0^\circ$). Therefore, it is absolutely natural that there will be a difference in the results of both outcomes for a single reaction on account of the change in the degree of freedom.

B. Analysis of the σ_{ff} and σ_{qf} cross sections

In this section, results for the fission region are discussed. Once the ΔR_{ER} has been fixed, then simultaneously ΔR_{ff}

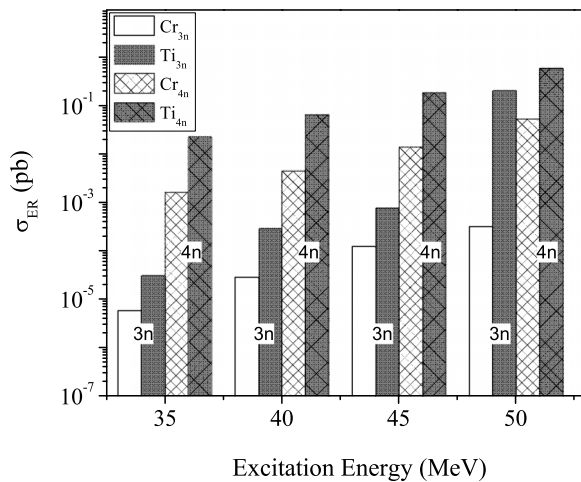


FIG. 4. DCM-predicted $\sigma_{3n,4n}$ cross sections within a comparison of two nuclei $^{302}120^*$ and $^{299}120^*$ at four energies. Solid+dark slabs in the case of $3n$ and $4n$ are showing Cr-induced and hollow slabs for $3n$ and $4n$ are for the Ti-induced reaction.

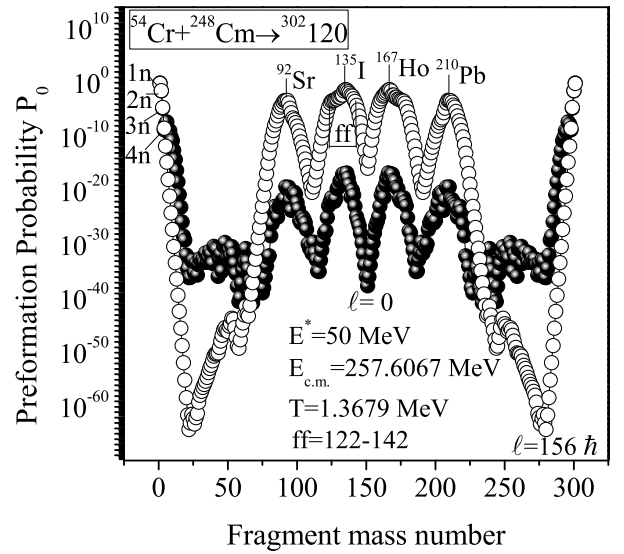


FIG. 5. Preformation probability (P_0) for the $^{54}\text{Cr} + ^{248}\text{Cm}$ reaction as a function of fragment mass A_i , $i = 1, 2$.

can also be calculated. During the decay process all the decay fragments, to some extent, influence each other's cross section and this effect helps to fix the ΔR 's. The present work follows the theoretical outline perfectly, i.e., the first step is the mutual capture of projectile and target nuclei, leading to the formation of a molecule-like nuclear system. After capture, the system evolves by exchanging nucleons. In the extreme case, the nuclei fuse and a compound nucleus (CN) is formed. The CN de-excites by evaporating nucleons or by fission. But the nuclear system can also re-separate before CN formation, thus resulting in quasifission (equivalent to a noncompound nucleus process).

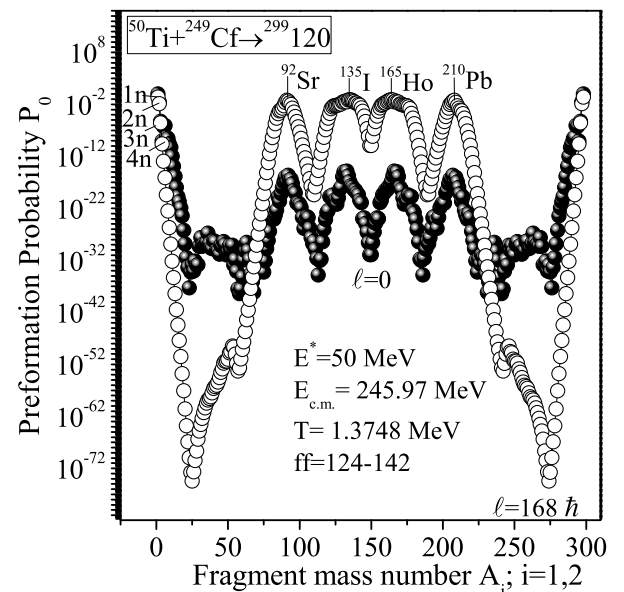


FIG. 6. Preformation probability (P_0) for $^{50}\text{Ti} + ^{249}\text{Cf}$ reaction as a function of fragment mass A_i , $i = 1, 2$.

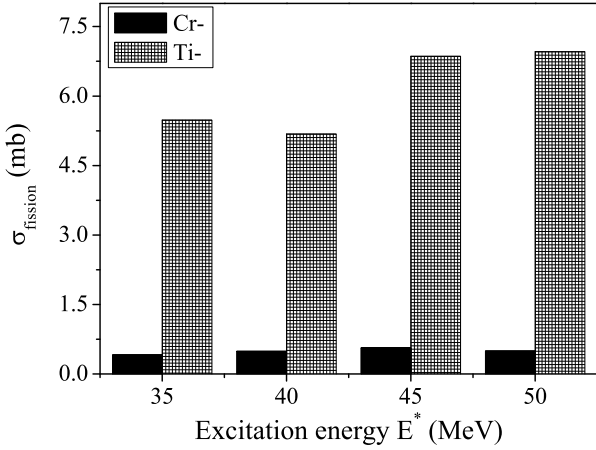


FIG. 7. Similarly as Fig. 5, but comparing σ_{ff} at all energies for both nuclei.

A special feature of the DCM is to describe the structure of the compound nucleus and it can be explained very well with the help of preformation probability (P_0). Due to the remaining shell effects at different temperatures, the calculated P_0 in Fig. 5 for the Cr-induced reaction within the hot fusion configurations shows maximal yields for the LPs (x neutrons, $x \leq 4$, ERs). Asymmetric fragments are centered around $A_L = 90-94$, $A_H = 208-212$ (the qf channel), and the regions of SF ($A = 122-142$) and peaks at $A_L = 135$, $A_H = 167$ (equivalently, $A/2 \pm 20$, the ff channel). Furthermore, in Fig. 6, the Ti-induced reaction shows the preformation distribution marked with maximal yields for LPs, asymmetric fragments were taken around $A_L = 87-94$, $A_H = 204-211$ (the qf channel), and similarly the peaks within the fission region ($A = 124-144$) at $A_L = 135$ and $A_H = 165$ (equivalently, $A/2 \pm 20$, the ff channel). From, Table III, shows the σ_{ff} and σ_{qf} predicted values and Fig. 7, explains the difference between the magnitude of the σ_{ff} of both reactions. After using the same potential barriers with the absolutely same ΔR values the output clearly shows a larger fission cross section in the case of the $^{50}\text{Ti} + ^{249}\text{Cf}$ reaction. Finally, we have estimated σ_{qf} , however, qf is a noncompound competing process where only the η_i contributes with the assumption of $P_0 = 1$. Although, it is difficult to calculate the quasifission without any experimental data, nevertheless, we tried to implement our idea to predict σ_{qf} . The calculation of σ_{qf} abides by the most general pattern found in the DCM studied cases, i.e., $\Delta R_{ER} > \Delta R_{qf} > \Delta R_{ff}$. ERs occur first having the largest ΔR , followed by the competing qf, and ending finally with ff of the hot CN (e.g., see Refs. [15,38,41]). In Table III, there is clear indication of increasing values of σ_{qf} with increasing energy. But the point to be emphasized is about the quasifission contribution in both reactions, i.e., the strength of σ_{qf} is higher in the case of the Cr-induced rather than the Ti-induced reaction.

The next important term to be calculated with all the predicted cross sections is the capture cross section (σ_{capture}). The capture cross section is the sum of qf, ff, and fusion-evaporation residue (ER) cross sections: $\sigma_{\text{capture}} = \sigma_{ER} + \sigma_{ff} + \sigma_{qf}$. For light nuclear systems, $\sigma_{\text{fusion}} \approx \sigma_{ER}$. However

TABLE III. DCM-predicted fission and quasifission cross sections ($\sigma_{qf,ff}^{\text{pred.}}$) with the distribution as $A_L = 90-94$, $A_H = 122-142$ in the case of $^{54}\text{Cr} + ^{248}\text{Cm} \rightarrow ^{302}120^*$, and $A_L = 87-95$, $A_H = 124-144$ for the $^{50}\text{Ti} + ^{249}\text{Cf} \rightarrow ^{299}120^*$ reaction. The second observation is for qf-cross section (or nCN) at four E^* values along with the P_{CN} .

Decay modes	ΔR (fm)	$\sigma_{qf,ff}^{\text{predicted}}$ (mb)	P_{CN}
$^{54}\text{Cr} + ^{248}\text{Cm} \rightarrow ^{302}120^*$			
$E^* = 50$ MeV			
90-94	0.126	8.63×10^{-03}	
122-142	0.256	0.492	
quasifission	0.55	191	0.006
$E^* = 45$ MeV			
90-94	0.124	9.03×10^{-03}	
122-142	0.254	0.56	
quasifission	0.5	85.8	0.007
$E^* = 40$ MeV			
90-94	0.122	6.83×10^{-03}	
122-142	0.252	0.49	
quasifission	0.282	18.5	0.026
$E^* = 35$ MeV			
90-94	0.12	4.92×10^{-03}	
122-142	0.25	0.41	
quasifission	0.15	17.8	0.022
$^{50}\text{Ti} + ^{249}\text{Cf} \rightarrow ^{299}120^*$			
$E^* = 50$ MeV			
87-94	0.126	2.01	
124-144	0.256	6.96	
quasifission	0.55	57	0.15
$E^* = 45$ MeV			
87-94	0.124	2.35	
124-144	0.254	6.98	
quasifission	0.5	39.4	0.19
$E^* = 40$ MeV			
87-94	0.122	2.96	
124-144	0.252	5.24	
quasifission	0.282	17.9	0.32
$E^* = 35$ MeV			
87-94	0.12	3.57	
124-144	0.25	5.52	
quasifission	0.15	12.6	0.42

in very heavy systems the strong Coulomb repulsion and large angular momenta lead to tiny probabilities for the CN formation. According to the results of model calculations, the reaction with the least quasifission component is more reasonable to produce $Z = 120$. The corresponding P_{CN} values at all energies are also listed here, which shows a clear inclination in the case of both nuclei at $E^* = 35-50$ MeV. The P_{CN} decreases as we move from lower to higher ener-

gies and, in the case of the Ti-induced compound nucleus formation, the probability is higher than for the Cr-induced reaction. The final evaluated result from all DCM-predicted cross sections shows the high probability of synthesizing $Z = 120$ via the $^{50}\text{Ti} + ^{249}\text{Cf}$ combination, in comparison to the $^{54}\text{Cr} + ^{248}\text{Cm}$ reaction. So, our present predicted results are encouraging for the $^{50}\text{Ti} + ^{249}\text{Cf}$ t-p combination. As given in the Introduction, a few studies have also predicted that the Ti-induced reactions can be considered for the synthesis of element 120 (see Refs. [5,8,9]). Our estimated results are also equivalent to these predictions in the case of Ti-induced reactions. Which increases our hope that a Ti beam could be a promising option to synthesis the compound nucleus $Z = 120$. Even so, without any strong evidence of experimental results, we cannot claim these predictions are correct, but these calculations may be helpful for making progress in the right direction for experimentalists. Model calculations are essential as a guideline for the experiments to find the optimum parameters as well as for the interpretation of the experimental results.

IV. SUMMARY AND CONCLUSIONS

In this paper, the fusion probability of the $^{54}\text{Cr} + ^{248}\text{Cm}$ and $^{50}\text{Ti} + ^{249}\text{Cf}$ reactions is examined at four energies using the DCM. This work has been done after cross-checking the predictive power of the model, but still without experimental verifications, it would be difficult to confirm the results. Here, the conjecture is about the predictive power of the neck-length parameter, which may be considerably helpful for future searches of superheavy elements. We have demonstrated the

decisive role of the neck-length parameter, which has been accepted as to provide hints in the appropriate direction in many cases. This work attempts the predicted quasifission for both nuclear reactions at all energies, although it is strenuous to predict σ_{qf} without knowing the contributions of all other decay channels. Therefore, the results are absolutely in line with the ideas taken from our previous studies using the DCM. We found a preference of the Ti-induced reaction for the synthesis of $Z = 120$. If a Ti beam is used instead of a Cr beam then chances are likely to increase. This extensive study is not enough to determine with absolute certainty the incoming channel for the production of $Z = 120$. One has also to search for alternative t-p combinations, which may be able to produce $Z = 120$. The present work may contribute to the design of future experiments for the synthesis of $Z = 120$.

ACKNOWLEDGMENTS

We thank Dr. S. Heinz from the GSI Helmholtz Centre for Heavy Ion Research, Darmstadt, Germany, who shared her experimental thoughts on superheavy elements with us in a very detailed manner. Also sincere thanks to Dr. Dorin N. Poenaru and Dr. R. A. Gherghescu for their guidance and contribution in discussions. Finally, our profound thanks to Prof. Dr. Horst Stöcker for his encouragements and hospitality at the FIAS. S.C. acknowledges support as a guest scientist under a Humboldt fellowship at the Frankfurt Institute of Advanced Studies and P.O.H. acknowledges financial support from “Dirección General de Asuntos del Personal Académico UNAM,” PAPIIT-DGAPA (IN116824).

-
- [1] S. Hofmann and G. Munzenberg, *Rev. Mod. Phys.* **72**, 733 (2000).
- [2] K. Morita, K. Morimoto, D. Kaji, T. Akiyama, S.-I. Goto, H. Haba, E. Ideguchi, K. Katori, H. Koura, H. Kudo, T. Ohnishi, A. Ozawa, T. Suda, K. Sueki, F. Tokanai, T. Yamaguchi, A. Yoneda, and A. Yoshida, *J. Phys. Soc. Jpn.* **76**, 043201 (2007).
- [3] S. Hofmann, S. Heinz, R. Mann, J. Maurer, G. Munzenberg, S. Antalic, W. Barth, H. G. Burkhard, L. Dahl, K. Eberhardt, R. Grzywacz, J. H. Hamilton, R. A. Henderson, J. M. Kenneally, B. Kindler, I. Kojouharov, R. Lang *et al.*, *Eur. Phys. J. A* **52**, 180 (2016).
- [4] V. I. Zagrebaev and W. Greiner, *Nucl. Phys. A* **944**, 257 (2015).
- [5] M.-H. Zhang, Y.-H. Zhang, Y. Zou, C. Wang, L. Zhu, and F.-S. Zhang, *Phys. Rev. C* **109**, 014622 (2024).
- [6] N. Wang, E. G. Zhao, W. Scheid, and S. G. Zhou, *Phys. Rev. C* **85**, 041601(R) (2012).
- [7] G. G. Adamian, N. V. Antonenko, W. Scheid, and V. V. Volkov, *Nucl. Phys. A* **633**, 409 (1998); G. Adamian and N. Antonenko, in *Clusters in Nuclei*, Vol. 2, Lecture Notes in Physics 848, edited by C. Beck (Springer Nature, 2012), p. 165.
- [8] H. M. Albers, J. Khuyagbaatar, D. J. Hinde, I. P. Carter, K. J. Cook, M. Dasgupta, C. E. Düllmann, K. Eberhardt *et al.*, *Phys. Lett. B* **808**, 135626 (2020).
- [9] J. Khuyagbaatar, A. Yakushev, Ch. E. Düllmann, D. Ackermann, L.-L. Andersson, M. Asai, M. Block, R. A. Boll, H. Brand, D. M. Cox *et al.*, *Phys. Rev. C* **102**, 064602 (2020).
- [10] S. Chopra, N. Goel, M. K. Sharma, P. O. Hess, and Hemdeep, *Phys. Rev. C* **106**, L031601 (2022).
- [11] S. Chopra, P. O. Hess, and M. K. Sharma, *Phys. Rev. C* **108**, L021601 (2023).
- [12] S. Chopra, M. K. Sharma, P. O. Hess, and J. Bedi, *Phys. Rev. C* **105**, 014610 (2022).
- [13] K. Wen, M. C. Barton, A. Rios, and P. D. Stevenson, *Phys. Rev. C* **98**, 014603(R) (2018).
- [14] V. Zagrebaev and W. Greiner, *J. Phys. G: Nucl. Part. Phys.* **31**, 825 (2005); V. Zagrebaev and W. Greiner, in *Clusters in Nuclei*, Vol. 1, Lecture Notes in Physics 818, edited by C. Beck (Springer Nature, 2010), p. 267.
- [15] R. K. Gupta, S. K. Arun, R. Kumar, and Niyti, *Int. Rev. Phys. (IREPHY)* **2**, 369 (2008).
- [16] R. K. Gupta, in *Clusters in Nuclei*, Lecture Notes in Physics 818, edited by C. Beck, Vol. I (Springer Verlag, Berlin, 2010), pp. 223–265, and earlier references there in it.
- [17] A. Sandulescu, D. N. Poenaru, and W. Greiner, *Sov. J. Part. Nucl.* **11**, 528 (1980).
- [18] M. Manhas and R. K. Gupta, *Phys. Rev. C* **72**, 024606 (2005).
- [19] R. K. Gupta, M. Balasubramaniam, C. Mazzocchi, M. L. Commara, and W. Scheid, *Phys. Rev. C* **65**, 024601 (2002).

- [20] R. K. Gupta, R. Kumar, N. K. Dhiman, M. Balasubramaniam, W. Scheid, and C. Beck, *Phys. Rev. C* **68**, 014610 (2003).
- [21] M. Balasubramaniam, R. Kumar, R. K. Gupta, C. Beck, and W. Scheid, *J. Phys. G: Nucl. Part. Phys.* **29**, 2703 (2003).
- [22] G. Royer and J. Mignen, *J. Phys. G: Nucl. Part. Phys.* **18**, 1781 (1992).
- [23] H. S. Khosla, S. S. Malik, and R. K. Gupta, *Nucl. Phys. A* **513**, 115 (1990).
- [24] S. Kumar and R. K. Gupta, *Phys. Rev. C* **55**, 218 (1997).
- [25] R. K. Gupta, S. Kumar, and W. Scheid, *Int. J. Mod. Phys. E* **6**, 259 (1997).
- [26] T. Matsuse, C. Beck, R. Nouicer, and D. Mahboub, *Phys. Rev. C* **55**, 1380 (1997).
- [27] S. J. Sanders, *Phys. Rev. C* **44**, 2676 (1991).
- [28] S. J. Sanders, D. G. Kovar, B. B. Back, C. Beck, D. J. Henderson, R. V. F. Janssens, T. F. Wang, and B. D. Wilkins, *Phys. Rev. C* **40**, 2091 (1989).
- [29] J. Błocki, J. Randrup, W. J. Swiatecki, and C. F. Tsang, *Ann. Phys. (NY)* **105**, 427 (1977).
- [30] B. B. Singh, M. K. Sharma, and R. K. Gupta, *Phys. Rev. C* **77**, 054613 (2008).
- [31] R. K. Gupta, N. Singh, and M. Manhas, *Phys. Rev. C* **70**, 034608 (2004).
- [32] R. K. Gupta, M. Balasubramaniam, R. Kumar, N. Singh, N. Manhas, and W. Greiner, *J. Phys. G: Nucl. Part. Phys.* **31**, 631 (2005).
- [33] R. K. Gupta, M. Manhas, and W. Greiner, *Phys. Rev. C* **73**, 054307 (2006).
- [34] R. K. Gupta, in *Proceedings of the 5th International Conference on Nuclear Reaction Mechanisms, Varenna, Italy*, edited by E. Gadioli (Ricerca Scientifica Educazione Permanente, Italy, 1988), p. 416.
- [35] S. S. Malik and R. K. Gupta, *Phys. Rev. C* **39**, 1992 (1989).
- [36] A. Kaur, S. Chopra, and R. K. Gupta, *Phys. Rev. C* **90**, 024619 (2014).
- [37] Niyti, G. Sawhney, M. K. Sharma, and R. K. Gupta, *Phys. Rev. C* **91**, 054606 (2015).
- [38] S. Chopra, Hemdeep, and R. K. Gupta, *Phys. Rev. C* **95**, 044603 (2017).
- [39] S. Chopra, M. Bansal, M. K. Sharma, and R. K. Gupta, *Phys. Rev. C* **88**, 014615 (2013).
- [40] S. Chopra, M. K. Sharma, P. O. Hess, Hemdeep, and NeetuMaan, *Phys. Rev. C* **103**, 064615 (2021).
- [41] R. K. Gupta, Niyti, M. Manhas, and S. Hoffman, *Int. J. Mod. Phys. E* **18**, 601 (2009).